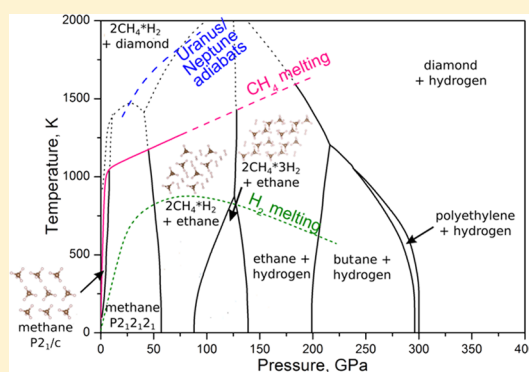


# Hydrocarbons under Pressure: Phase Diagrams and Surprising New Compounds in the C–H System

Anastasia S. Naumova,<sup>\*,†,‡,§,||</sup> Sergey V. Lepeshkin,<sup>†,§,||</sup> and Artem R. Oganov<sup>†,‡,||</sup><sup>†</sup>Skolkovo Institute of Science and Technology, Skolkovo Innovation Center, 3 Nobel Street, Moscow 121205, Russian Federation<sup>‡</sup>Moscow Institute of Physics and Technology, 9 Institutskiy Lane, Dolgoprudny, Moscow Region 141700, Russian Federation<sup>§</sup>Lebedev Physical Institute, Russian Academy of Sciences, 119991 Leninskii Avenue 53, Moscow, Russia<sup>||</sup>International Center for Materials Discovery, Northwestern Polytechnical University, Xi'an 710072, China

## Supporting Information

**ABSTRACT:** Understanding the high-pressure behavior of the C–H system is of great importance due to its key role in organic, bio-, petroleum, and planetary chemistry. We have performed a systematic investigation of the pressure–composition phase diagram of the C–H system at pressures up to 400 GPa using evolutionary structure prediction coupled with ab initio calculations and discovered that only saturated hydrocarbons are thermodynamically stable. Several stable methane–hydrogen cocrystals are predicted:  $2\text{CH}_4 * \text{H}_2$ , earlier obtained experimentally, is predicted to have the  $I4/m$  space group and 2–90 GPa stability range at 0 K, and two new thermodynamically stable compounds  $2\text{CH}_4 * 7\text{H}_2$  ( $P-3m1$  space group) and  $\text{CH}_4 * 9\text{H}_2$  ( $Cm$  space group), and are potential energy storage materials. The  $P2_1/c$  phase of methane is predicted to be stable at pressures <8 GPa; bulk graphane (CH) was shown to be thermodynamically stable at 7–18 and 18–50 GPa and 0 K in the  $P-3m$  and  $Cmca$  phases, respectively; polyethylene is shown to have a narrow field of stability. We report the  $p$ – $T$ – $x$  phase diagram of the C–H system and  $p$ – $T$  phase diagram of  $\text{CH}_4$ .



## INTRODUCTION

Hydrocarbons are of great interest due to their importance in many fields, such as organic chemistry, planetary science, and others.<sup>1,2</sup> For instance, they play a key role in giant planets such as Neptune and Uranus. Today's models of these planets postulate a three-layered structure, consisting of an inner rocky core, middle ice layer of compounds of C, N, H, and O, and an outer H–He atmosphere.<sup>3</sup> The abundance of methane in the ice layer is quite high (up to 30 mass %, depending on the model used) at pressures up to several hundreds of GPa.<sup>4</sup> In previous works,<sup>5–7</sup> it was shown that ethane, butane, and polymeric hydrocarbons are also likely to exist under conditions corresponding to the middle layer. However, in one theoretical paper, the stability of butane was questioned.<sup>8</sup> Later, we will come back to this issue and show that the chemistry of this middle layer is surprisingly diverse. Interestingly, Neptune has unexplained internal heat production responsible for its high luminosity. One of the possible explanations is that, at high pressures, methane decomposes into hydrogen and diamond.<sup>6,7,9–14</sup> The latter is denser than hydrocarbons and hydrogen and, therefore, gravitationally sinks inside the planet.<sup>15</sup> Most likely this process involves multiple stages, and several intermediate compounds are produced during methane polymerization. In agreement with this consideration is the fact that methane, ethane, and butane

cannot sink and may leak into the atmosphere where  $\text{CH}_4$  and  $\text{C}_2\text{H}_6$  were indeed found there.<sup>16</sup>

Another interesting fact about C–H compounds comes from organic chemistry: benzene ( $\text{C}_6\text{H}_6$ ) has been known for a long time, but its thermodynamically more stable isomer graphane,<sup>17,18</sup> that is,  $(\text{CH})_\infty$ , was discovered experimentally just in 2009,<sup>19</sup> and recently, bulk graphane was also synthesized.<sup>20</sup> Can there be other stable, but as yet unknown, hydrocarbons?

We have made an attempt to answer this question and found that, despite its great importance, the phase diagram of the C–H system is poorly known. At ambient pressure, only methane lies on the convex hull (all other hydrocarbons are thermodynamically unstable and have a higher free energy than a mixture of graphite, hydrogen, and methane); above 4 GPa, it was shown experimentally that it forms different cocrystals with  $\text{H}_2$ ,<sup>21</sup> which normally decompose when pressure is raised beyond several GPa. Theoretical predictions show one remarkable exception:  $2\text{CH}_4 * 3\text{H}_2$  that was found to be stable at pressures up to 215 GPa.<sup>22</sup> Methane itself adopts several phases obtained experimentally, but the

Received: February 12, 2019

Revised: July 24, 2019

Published: July 25, 2019

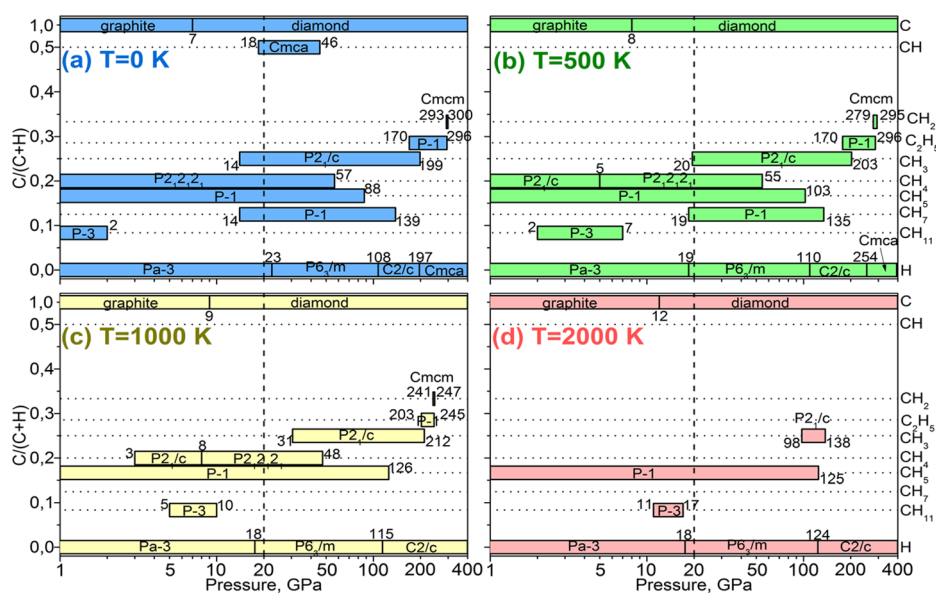


**Figure 1.** Pressure–composition phase diagram representation of C–H system at 0–400 GPa calculated using optB88-vdW (at 1–20 GPa) and PBE (at 20–400 GPa) functionals at (a) 0 K with zero-point energy included, (b) 500 K, (c) 1000 K, and (d) 2000 K. CH = graphane; CH<sub>2</sub> = polyethylene; C<sub>2</sub>H<sub>5</sub> = butane; CH<sub>3</sub> = ethane; CH<sub>4</sub> = methane; CH<sub>5</sub> = 4CH<sub>4</sub> \* 2H<sub>2</sub>; CH<sub>7</sub> = 2CH<sub>4</sub> \* 3H<sub>2</sub>; CH<sub>11</sub> = 2CH<sub>4</sub> \* 7H<sub>2</sub>.

structures of some of them remain unidentified.<sup>23,24</sup> At pressures above 155 GPa, pure methane was predicted to decompose into a mixture of hydrogen and ethane, and at still higher pressures, butane and polyethylene were predicted to form.<sup>5</sup> Further pressure increase leads to the formation of diamond and hydrogen.<sup>9</sup> On the other hand, as a result of experimental studies, methane was reported to remain stable at room temperature and compression up to 200 GPa (but note that it can be metastable at such low temperature as 300 K).<sup>25</sup> Another static compression experiment showed its stability up to 80 GPa and 2000 K.<sup>26</sup>

Only two systematic theoretical studies of compound stability in the C–H system under pressure were done.<sup>5,8</sup> In those works, the authors used a fixed-composition search that did not allow finding phases with unusual compositions because compositions have to be manually set. We have addressed this with the recently developed variable-composition search, introduced in USPEX,<sup>27,28</sup> which performs simultaneous prediction of all stable stoichiometries and structures (in a given range of compositions) automatically, in combination with accurate DFT calculations. This method proved to be successful for predicting various novel materials.<sup>29</sup> As a result, we report the full phase diagram of the C–H system at pressures of 0–400 GPa and temperatures from 0 up to 2000 K.

## METHODS

The USPEX method<sup>27,28</sup> is based on the evolutionary algorithm and operates as the following: the first generation of structures is created randomly and then relaxed; some predefined percentage of energetically best structures acts as “parents” for the next generation, which is produced by means of so-called variational operators (mutations, crossover, and random structure generators) and also locally optimized; this procedure is repeated until the global minimum is found. The variable-composition method allowed us to search for all stable states in the C–H system. USPEX searches were performed with 8–32 atoms per unit cell at pressures 0, 1, 2, ..., 10, 12, 14,

..., 20, 40, 60, ..., 100, 150, 200, ..., 400 GPa and involved more than 200000 structure relaxations. Total energy calculations and structure relaxations were performed using the PBE functional and the PAW method,<sup>30–32</sup> with hard potentials, 850 eV plane wave kinetic energy cutoff, and a uniform  $\Gamma$ -centered grid with  $2\pi \times 0.056 \text{ \AA}^{-1}$  spacing for reciprocal space sampling. We also used optB88-vdW functional with van der Waals correction at pressures of 0–20 GPa, when dispersion interactions are still important,<sup>33</sup> and SCAN functional with rVV10 correction and 1000 eV plane wave kinetic energy cutoff.<sup>34</sup> All structure relaxations and total energy calculations were done using the VASP code.<sup>35</sup> For all calculations with vdW corrections, a less dense  $\Gamma$ -centered grid was applied, that is,  $2\pi \times 0.064 \text{ \AA}^{-1}$ , as it was done in Saleh and Oganov’s work.<sup>22</sup>

For thermodynamically stable structures, phonon dispersion curves, phonon density of states, and phonon contribution to the free energy were calculated using the finite displacement method as implemented in the PHONOPY code.<sup>36</sup> The dynamical stability of novel compounds was ascertained by the absence of imaginary frequencies in their phonon dispersion curves. Large supercells ( $\sim 10 \times 10 \times 10 \text{ \AA}$ ) and increased energy cutoff (1000 eV) were adopted in order to avoid artificial imaginary frequencies. In the case of *P*-3*m*1-graphane, a very large supercell ( $6 \times 6 \times 4, 15 \times 13 \times 16 \text{ \AA}$ , 576 atoms) was needed. The pressure–composition and pressure–temperature phase diagrams were obtained using the computed Gibbs free energies at given pressure and temperature in the quasiharmonic approximation; thermal expansion was taken into account. The chosen approach was validated by a number of studies where phase diagrams of various materials were calculated (e.g., Ref. 37–39).

## RESULTS AND DISCUSSION

We calculated the phase diagram of the C–H system at 1–400 GPa with and without vdW corrections (optB88-vdW and PBE functionals, respectively) and with and without zero-point energy. Also, one more re-calculation of the whole pressure–

composition phase diagram was done using the SCAN functional (see the [Supporting Information](#) for additional picture representations).<sup>34</sup> Results obtained with these functionals are quite similar and differ in exact stability pressure intervals; the more significant changes will be discussed below. Further in the text, we will consider calculations with vdW correction up to 20 GPa, without it at pressures more than 20 GPa, and always including ZP energy, unless stated otherwise. Using all predicted stable structures, we have computed phase diagrams at different temperatures: 500, 1000, and 2000 K ([Figure 1](#)).

All stable compounds discovered in previous structure prediction works were reproduced in our simulations,<sup>5–8,22</sup> and a number of new stable compounds were predicted. The corresponding most stable carbon (graphite and diamond) and hydrogen phases were predicted similar to reference.<sup>22</sup> We found that there are no stable unsaturated (including aromatic) hydrocarbons on the phase diagram. Another interesting fact that comes from our calculations is that several methane-hydrogen cocrystals are thermodynamically stable and have a wide stability range. Further, we will review obtained compounds, which are newly discovered or have some differences in comparison with previous studies (their structures are shown in [Figure 2](#)).

Butane  $C_4H_{10}$  has the  $P-1$  space group, and its thermodynamic and dynamical stability is debated in the literature.<sup>5,8</sup> According to our results, at 0 K, butane is present on the phase diagram from 170 to 296 GPa, and it remains thermodynamically stable at temperatures up to 1200 K. This confirms results of Gao et. al.,<sup>5</sup> and disagrees with Liu et. al.<sup>8</sup>

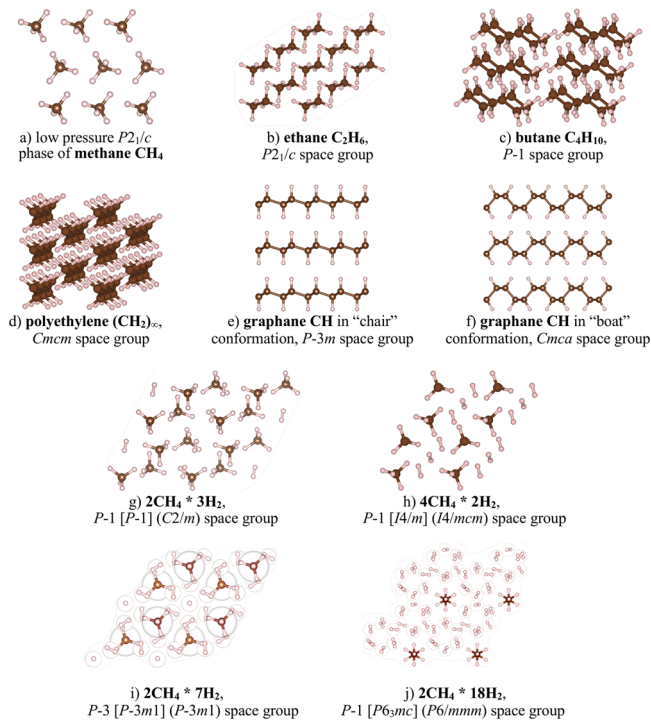


**Figure 2.** Structures of predicted compounds with their space groups. Spheres indicate spherical symmetry of the molecule inside and are shown only in those cases where they help to determine higher symmetry. Space groups in square brackets were determined considering all molecules to be spherical (with centers in their centers of mass), while those in round brackets were determined considering only carbons.

Polyethylene  $(CH_2)_\infty$  has the  $Cmcm$  space group and is thermodynamically stable (with no ZPE correction included) at pressures above 130 GPa but is extremely close to the convex hull at all pressures, and for this reason, it was previously reported to have three ranges of stability: <20, 140–190, and >215 GPa.<sup>22</sup> In our calculations, polyethylene  $(CH_2)_\infty$  at some pressures is just 0.2–0.6 meV/atom above the convex hull. When taking into account zero-point energy, polyethylene turns out to have a very narrow stability region on the phase diagram ([Figure 2a–c](#)) at different temperatures.<sup>5,8</sup>

Also, it was shown that two phases of bulk graphane with  $P-3m$  (corresponds to the chair conformation of its single unit, namely, the six-membered carbon ring) and  $Cmca$  (corresponds to the boat conformation) space groups are thermodynamically stable (graphane I and III in ref 18) if vdW correction is not taken into account. In this case, both these phases have no imaginary phonon frequencies and exist at 7–18 and 18–50 GPa at 0 K, respectively. When vdW correction is included, the  $P-3m$  phase become unstable. In the experimental work by Kondrin et al.,<sup>20</sup> graphane was obtained from benzene at 8–10 GPa and 900–1000 K as a partially crystallized material; the authors mentioned that, at higher pressure, the degree of crystallization is expected to be higher, which is consistent with our results.

In the experimental work by Somayazulu et al., the  $4CH_4 * 2H_2$  cocrystal with space group  $I4/mcm$  was reported to be stable in the range from 5.4 GPa to >30 GPa.<sup>21</sup> In our work, we also obtained a structure with the same C/H ratio and space group  $I4/m$  (considering all molecules as spheres, [Figure 2b](#)) or  $I4/mcm$  (if only methane centers of mass are considered, which is reasonable due to the fact that, in X-ray diffraction experiments, positions of hydrogen atoms at high pressure are not determined well), which is in good agreement with experimental results.<sup>21</sup> This structure is stable from 2 up to ~90 GPa at 0 K and remains stable even at high temperatures ([Figures 1](#) and [3](#)) up to about 150 GPa and 2000 K (at 3000 K, only diamond and hydrogen are stable) when pure methane turns out to be not stable anymore.

We also found two new methane-hydrogen cocrystals:  $2CH_4 * 7H_2$  and  $CH_4 * 9H_2$ .  $2CH_4 * 7H_2$  adopts the  $P-3$  space group or  $P-3m1$  if  $H_2$  and  $CH_4$  have spherical symmetries

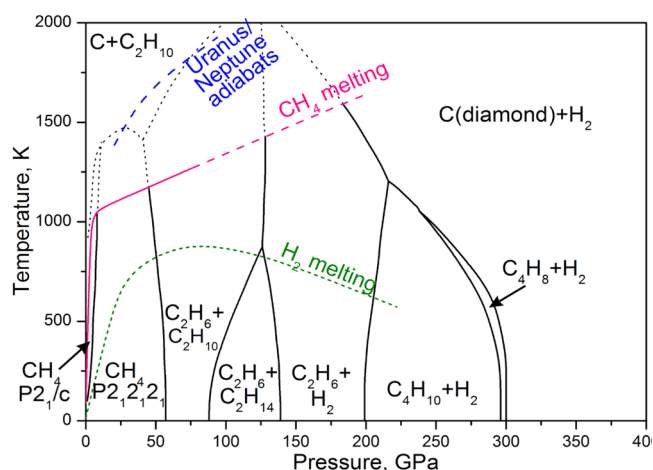
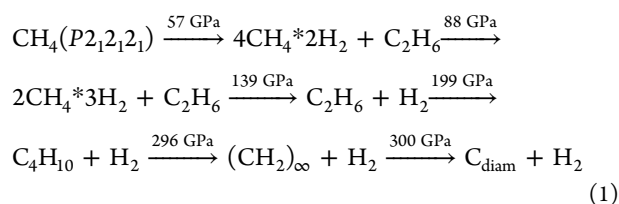


**Figure 3.** Phase diagram of  $CH_4$ . The melting line of  $CH_4$  comes from ref 41, and that of  $H_2$  comes from ref 42. Uranus/Neptune adiabats are from ref 43; dashed lines indicate melting line approximations by the Simon–Glatzel equation.<sup>43</sup>

(Figure 2i), and  $\text{CH}_4 * 9\text{H}_2$  adopts the  $P-1$  space group or  $P6_3/mc$  considering spherical symmetry of all molecules (Figure 2j). Both structures were initially found with the SCAN functional, and then these were re-calculated using optB88-vdw and PBE functionals. When ZPE is included,  $2\text{CH}_4 * 7\text{H}_2$  is located on the convex hull. We expect experimental synthesis of this compound to be possible. Potentially,  $2\text{CH}_4 * 7\text{H}_2$  can be used as a very effective hydrogen-storage material due to its wide temperature and low-pressure stability ranges and high hydrogen content, about 30 mass % (a little less than that of H4M ( $\text{CH}_4 * 4\text{H}_2$ ),<sup>21</sup> the most hydrogen-rich chemical compound known for now – but, unfortunately, existing only at high pressure).  $\text{CH}_4 * 9\text{H}_2$  becomes unstable when ZPE is added.

A special point is the study of methane. Figure 3 shows the total  $p$ – $T$  phase diagram of  $\text{CH}_4$ . According to our results, methane undergoes the following transformations with increasing pressure at  $T = 0$  K toward diamond formation (the process that is believed to proceed in giant planets' interiors):



We found the  $P_{2,2,2,1}$  phase of methane (Figure 2a) to be stable in the pressure range up to 8 GPa at finite temperatures. If vdW correction is not included, this phase is stable even at 0 K up to 8 GPa.

In contradiction with previous theoretical works,<sup>5,22</sup> we show that, starting from 60 GPa, pure methane becomes unstable at 0 K, so the  $Pnma$  phase from work by Gao et al.<sup>5</sup> is not on the phase diagram anymore at any temperature and pressure since it decomposes to  $4\text{CH}_4 * 2\text{H}_2$  and ethane and then to  $2\text{CH}_4 * 3\text{H}_2$  and ethane (as seen from Figure 3). These decomposition reactions could only be predicted in this work due to the use of variable-composition USPEX code. All transition pressures between different phases on the  $p$ – $T$  phase diagram were re-calculated more precisely than it was done in previous works. Liu et al. in their calculations obtained similar results for  $\text{CH}_4$  as we did at 200 and 300 GPa but different at 100 GPa since the  $2\text{CH}_4 * 3\text{H}_2$  phase was not taken into account.<sup>8</sup> The appearance of  $2\text{CH}_4 * 3\text{H}_2$  and  $4\text{CH}_4 * 2\text{H}_2$  cocrystals together with ethane on the  $p$ – $T$  phase diagram is also a new result of our work, which is consistent with experimental results<sup>40</sup> where methane, ethane, and hydrogen coexist at high-pressure conditions, though the stability pressure range is slightly different.

## CONCLUSIONS

In conclusion, we have shown that, for the C–H system, only saturated hydrocarbons, namely, alkanes, are thermodynamically stable and there are no stable unsaturated compounds because the  $\pi$  bonds of any multiple bonds are energetically less favorable than a single bond.<sup>17</sup> We have studied the full phase diagram of the C–H system in wide ranges of temperature (up to 3000 K) and pressure (up to 400 GPa) and found that several methane-hydrogen cocrystals are thermodynamically stable. Several new structures were explored during our studies: cocrystal  $2\text{CH}_4 * \text{H}_2$ , earlier

obtained experimentally, was discovered to have the  $I4/m$  (or  $I4/mcm$  if only carbons are considered) space group and 2–90 GPa stability range at 0 K. The  $P_{2,2,2,1}$  phase of methane was discovered to be stable at low pressures; bulk graphane (CH) was shown to be thermodynamically stable at 18–50 GPa and 0 K with the  $Cmca$  space group; polyethylene was found on the phase diagram in a narrow range. Two new methane hydrogenates  $2\text{CH}_4 * 7\text{H}_2$  ( $P-3m1$  space group) and  $\text{CH}_4 * 9\text{H}_2$  ( $Cm$  space group) were discovered that can possibly be used for hydrogen-storage purposes.

## ASSOCIATED CONTENT

### Supporting Information

The Supporting Information is available free of charge on the ACS Publications website at DOI: 10.1021/acs.jpcc.9b01353.

Additional C–H phase diagram representations calculated with different methods, convex hulls, structures of new compounds, phonon dispersion curves and phonon density of states (PDF)

## AUTHOR INFORMATION

### Corresponding Author

\*E-mail: naumova.nastasiya@gmail.com.

### ORCID

Anastasia S. Naumova: 0000-0002-8337-095X

Sergey V. Lepeshkin: 0000-0003-0155-8148

Artem R. Oganov: 0000-0002-9315-1419

### Notes

The authors declare no competing financial interest.

## ACKNOWLEDGMENTS

We acknowledge Valery V. Roizen and Efim A. Mazhnik for their kind methodological advices. Calculations were performed on our Rurik supercomputer, the Arkuda supercomputer of Skolkovo Foundation, and at the supercomputer center of the University of Nizhny Novgorod. We thank the Russian Science Foundation (grant 19-72-30043) for supporting this work.

## REFERENCES

- (1) Hazen, R. M.; Hemley, R. J.; Mangum, A. J. Carbon in Earth's Interior: Storage, Cycling, and Life. *Trans., Am. Geophys. Union* **2012**, *93*, 17–18.
- (2) Schlapbach, L.; Züttel, A. Hydrogen-storage materials for mobile applications. *Nature* **2001**, *414*, 353–358.
- (3) Hubbard, W. B.; MacFarlane, J. J. Structure and evolution of Uranus and Neptune. *J. Geophys. Res.: Solid Earth* **1980**, *85*, 225–234.
- (4) Hubbard, W. B.; Nellis, W. J.; Mitchell, A. C.; Holmes, N. C.; Limaye, S. S.; McCandless, P. C. Interior Structure of Neptune: Comparison with Uranus. *Science* **1991**, *253*, 648–651.
- (5) Gao, G.; Oganov, A. R.; Ma, Y.; Wang, H.; Li, P.; Li, Y.; Iitaka, T.; Zou, G. Dissociation of methane under high pressure. *J. Chem. Phys.* **2010**, *133*, 144508.
- (6) Ancilotto, F.; Chiarotti, G. L.; Scandolo, S.; Tosatti, E. Dissociation of Methane into Hydrocarbons at Extreme (Planetary) Pressure and Temperature. *Science* **1997**, *275*, 1288–1290.
- (7) Benedetti, L. R.; Nguyen, J. H.; Caldwell, W. A.; Liu, H.; Kruger, M.; Jeanloz, R. Dissociation of  $\text{CH}_4$  at High Pressures and Temperatures: Diamond Formation in Giant Planet Interiors? *Science* **1999**, *286*, 100–102.
- (8) Liu, H.; Naumov, I. I.; Hemley, R. J. Dense Hydrocarbon Structures at Megabar Pressures. *J. Phys. Chem. Lett.* **2016**, *7*, 4218–4222.

- (9) Zerr, A.; Serghiou, G.; Boehler, R.; Ross, M. Decomposition of alkanes at high pressures and temperatures. *High Pressure Res.* **2006**, *26*, 23–32.
- (10) Nellis, W. J.; Hamilton, D. C.; Mitchell, A. C. Electrical conductivities of methane, benzene, and polybutene shock compressed to 60 GPa (600 kbar). *J. Chem. Phys.* **2001**, *115*, 1015–1019.
- (11) Nellis, W. J.; Ree, F. H.; van Thiel, M.; Mitchell, A. C. Shock compression of liquid carbon monoxide and methane to 90 GPa (900 kbar). *J. Chem. Phys.* **1981**, *75*, 3055–3063.
- (12) Ross, M.; Ree, F. H. Repulsive forces of simple molecules and mixtures at high density and temperature. *J. Chem. Phys.* **1980**, *73*, 6146–6152.
- (13) Spanu, L.; Donadio, D.; Hohl, D.; Schwegler, E.; Galli, G. Stability of hydrocarbons at deep Earth pressures and temperatures. *Proc. Natl. Acad. Sci. U. S. A.* **2011**, *108*, 6843–6846.
- (14) Kolesnikov, A.; Kutcherov, V. G.; Goncharov, A. F. Methane-derived hydrocarbons produced under upper-mantle conditions. *Nat. Geosci.* **2009**, *2*, 566–570.
- (15) Ross, M. The ice layer in Uranus and Neptune – Diamonds in the sky? *Nature* **1981**, *292*, 435–436.
- (16) Moses, J. I.; Rages, K.; Pollack, J. B. An Analysis of Neptune's Stratospheric Haze Using High-Phase-Angle Voyager Images. *Icarus* **1995**, *113*, 232–266.
- (17) Wen, X.-D.; Hoffmann, R.; Ashcroft, N. W. Benzene under High Pressure: a Story of Molecular Crystals Transforming to Saturated Networks, with a Possible Intermediate Metallic Phase. *J. Am. Chem. Soc.* **2011**, *133*, 9023–9035.
- (18) Wen, X.-D.; Hand, L.; Labet, V.; Yang, T.; Hoffmann, R.; Ashcroft, N. W.; Oganov, A. R.; Lyakhov, A. O. Graphane sheets and crystals under pressure. *Proc. Natl. Acad. Sci. U. S. A.* **2011**, *108*, 6833–6837.
- (19) Elias, D. C.; Nair, R. R.; Mohiuddin, T. M. G.; Morozov, S. V.; Blake, P.; Halsall, M. P.; Ferrari, A. C.; Boukhvalov, D. W.; Katsnelson, M. I.; Geim, A. K.; et al. Control of Graphene's Properties by Reversible Hydrogenation: Evidence for Graphane. *Science* **2009**, *323*, 610–613.
- (20) Kondrin, M. V.; Nikolaev, N. A.; Boldyrev, K. N.; Shulga, Y. M.; Zibrov, I. P.; Brazhkin, V. V. Bulk graphanes synthesized from benzene and pyridine. *CrystEngComm* **2017**, *19*, 958–966.
- (21) Somayazulu, M. S.; Finger, L. W.; Hemley, R. J.; Mao, H. K. High-Pressure Compounds in Methane-Hydrogen Mixtures. *Science* **1996**, *271*, 1400–1402.
- (22) Saleh, G.; Oganov, A. R. Novel Stable Compounds in the C-H-O Ternary System at High Pressure. *Sci. Rep.* **2016**, *6*, 32486.
- (23) Bini, R.; Pratesi, G. High-pressure infrared study of solid methane: Phase diagram up to 30 GPa. *Phys. Rev. B* **1997**, *55*, 14800–14809.
- (24) Bini, R.; Ulivi, L.; Jodl, H. J.; Salvi, P. R. High pressure crystal phases of solid CH<sub>4</sub> probed by Fourier transform infrared spectroscopy. *J. Chem. Phys.* **1995**, *103*, 1353–1360.
- (25) Sun, L.; Yi, W.; Wang, L.; Shu, J.; Sinogeikin, S.; Meng, Y.; Shen, G.; Bai, L.; Li, Y.; Liu, J.; Mao, H.-k.; Mao, W. L. X-ray diffraction studies and equation of state of methane at 202 GPa. *Chem. Phys. Lett.* **2009**, *473*, 72–74.
- (26) Lobanov, S. S.; Chen, P.-N.; Chen, X.-J.; Zha, C.-S.; Litasov, K. D.; Mao, H.-K.; Goncharov, A. F. Carbon precipitation from heavy hydrocarbon fluid in deep planetary interiors. *Nat. Commun.* **2013**, *4*, 2446.
- (27) Oganov, A. R.; Glass, C. W. Crystal structure prediction using *ab initio* evolutionary techniques: Principles and applications. *J. Chem. Phys.* **2006**, *124*, 244704.
- (28) Oganov, A. R.; Lyakhov, A. O.; Valle, M. How Evolutionary Crystal Structure Prediction Works – and Why. *Acc. Chem. Res.* **2011**, *44*, 227–237.
- (29) Oganov, A. R.; Pickard, C. J.; Zhu, Q.; Needs, R. J. Structure prediction drives materials discovery. *Nat. Rev. Mater.* **2019**, *4*, 331–348.
- (30) Perdew, J. P.; Burke, K.; Ernzerhof, M. Generalized gradient approximation made simple. *Phys. Rev. Lett.* **1996**, *77*, 3865–3868.
- (31) Blöchl, P. E. Projector augmented-wave method. *Phys. Rev. B* **1994**, *50*, 17953–17979.
- (32) Kresse, G.; Joubert, D. From ultrasoft pseudopotentials to the projector augmented-wave method. *Phys. Rev. B* **1999**, *59*, 1758–1775.
- (33) Klimeš, J.; Bowler, D. R.; Michaelides, A. Van der Waals density functionals applied to solids. *Phys. Rev. B* **2011**, *83*, 195131.
- (34) Peng, H.; Yang, Z.-H.; Perdew, J. P.; Sun, J. Versatile van der Waals density functional based on a meta-generalized gradient approximation. *Phys. Rev. X* **2016**, *6*, No. 041005.
- (35) Kresse, G.; Furthmüller, J. Efficiency of *ab-initio* total energy calculations for metals and semiconductors using a plane-wave basis set. *Comput. Mater. Sci.* **1996**, *6*, 15–50.
- (36) Togo, A.; Tanaka, I. First principles phonon calculations in materials science. *Scr. Mater.* **2015**, *108*, 1–5.
- (37) Shorikov, A. O.; Roizen, V. V.; Oganov, A. R.; Anisimov, V. I. Role of temperature and Coulomb correlation in the stabilization of the CsCl-type phase in FeS under pressure. *Phys. Rev. B* **2018**, *98*, No. 094112.
- (38) Kvashnin, A. G.; Zakaryan, H. A.; Zhao, C.; Duan, Y.; Kvashnina, Y. A.; Xie, C.; Dong, H.; Oganov, A. R. New Tungsten Borides, Their Stability and Outstanding Mechanical Properties. *J. Phys. Chem. Lett.* **2018**, *9*, 3470–3477.
- (39) Oganov, A. R.; Gillan, M. J.; Price, G. D. Structural stability of silica at high pressures and temperatures. *Phys. Rev. B* **2005**, *71*, No. 064104.
- (40) Hirai, H.; Konagai, K.; Kawamura, T.; Yamamoto, Y.; Yagi, T. Polymerization and diamond formation from melting methane and their implications in ice layer of giant planets. *Phys. Earth Planet. Inter.* **2009**, *174*, 242–246.
- (41) Deemyad, S.; Silvera, I. F. Melting line of hydrogen at high pressures. *Phys. Rev. Lett.* **2008**, *100*, 155701.
- (42) De Pater, I.; Lissauer, J. J. *Planetary Sciences*; Cambridge University Press: Cambridge, U.K., 2001, p. 215.
- (43) Simon, F.; Glatzel, G. Bemerkungen zur Schmelzdruckkurve. *Z. Anorg. Allg. Chem.* **1929**, *178*, 309–316.